ELSEVIER

Chemical Engineering Journal 137 (2008) 561–567

Chemical Engineering Journal

www.elsevier.com/locate/cej

Reactivity of highly cycled particles of CaO in a carbonation/calcination loop

Gemma S. Grasa [a,*], J. Carlos Abanades [b], Mónica Alonso [b], Belén González [b]

[a] *Instituto de Carboquímica, CSIC, Miguel Luesma Castán 4, 50015 Zaragoza, Spain*
[b] *Instituto Nacional del Carbón, CSIC, Francisco Pintado Fe 26, 33011 Oviedo, Spain*

Received 5 February 2007; received in revised form 14 May 2007; accepted 15 May 2007

Abstract

Calcium oxide can be an effective sorbent for separating CO_2 at high temperatures. The carbonation reaction is the basis for several proposed high temperature CO_2 capture systems when coupled with a calcination step to produce a pure CO_2 stream. Fresh calcined lime is known to be able to carbonate very readily at appropriate temperatures, but the average sorbent particle in a capture system using CaO as regenerable sorbent has to undergo many carbonation/calcination cycles. This work investigates the carbonation reaction rates in highly cycled sorbent particles of CaO (20–100 s of carbonation/calcination cycles). A basic reaction model (homogeneous model) has been proved to be sufficient for interpreting the reactivity data obtained under different conditions: partial pressure of CO_2, particle sizes and other relevant operation variables for the carbonation/calcination loop. The intrinsic rate parameter was found to be between 3.2 and 8.9×10^{-10} $m^4/mol\,s$ in agreement with other values found in the literature.

Keywords: Limestone; CO_2 capture; Regenerable sorbent; Carbonation; Kinetics

1. Introduction

The separation of a pure CO_2 stream, combined with an efficiently managed geological storage site is considered to be a major mitigation option for climate change [1]. This solution could be applied using existing technologies, because many of the components in these systems are already commercially available. However, it is widely accepted that there is large scope for cost reduction and energy efficiency improvements in CO_2 capture systems. From the different approaches available for capturing CO_2, we focus in this paper on the separation of CO_2 from a flue gas stream using regenerable solid sorbents based on the carbonation/calcination loop of $CaO/CaCO_3$. The basic scheme of the process proposed is depicted in Fig. 1. Proposed by Shimizu et al. [2], it has been the subject of detailed analysis elsewhere [3,4]. The system consists of a carbonation reactor where a flue gas stream from a power plant meets a flux of CaO ready to react with the CO_2 present in the gas to form $CaCO_3$. A second reactor is used for the regeneration of the sorbent (calcination of $CaCO_3$). There are other options for the capture process proposed depending on the reactor type and the energy source employed to drive the regeneration of the sorbent. A common feature of all the options is the very low efficiency penalties that can be achieved due to the recovery (during the carbonation step at around 650 °C) of some of the energy supplied by the fuel used to regenerate the sorbent [3,4]. The low cost of the raw sorbent make-up (crushed limestone) and the possibility of using the calcined purge as a cement feedstock are also potential advantages that ensure very low CO_2 capture costs.

One of the critical units in these CO_2 capture systems is the carbonator reactor itself. High reaction rates between the CO_2 in the flue gas and the sorbent particles are necessary in order to design compact absorbers. Fresh calcined lime is known to be able to carbonate very readily at appropriate temperatures, but the average sorbent particle in the system must experience many carbonation/calcination cycles [4] and sorbent capture capacity will decrease rapidly in these conditions. Previous studies that have investigated the reversibility of the carbonation/calcination reaction have shown that carbonation is far from reversible in practice [2,5–10]. After a fast, chemically controlled, initial reaction stage, a second slower reaction stage controlled by diffusion in the product layer, $CaCO_3$, takes place [8]. It was also

* Corresponding author. Tel.: +34 976733977; fax: +34 976733318.
E-mail address: gga@carbon.icb.csic.es (G.S. Grasa).

1385-8947/$ – see front matter © 2007 Elsevier B.V. All rights reserved.
doi:10.1016/j.cej.2007.05.017

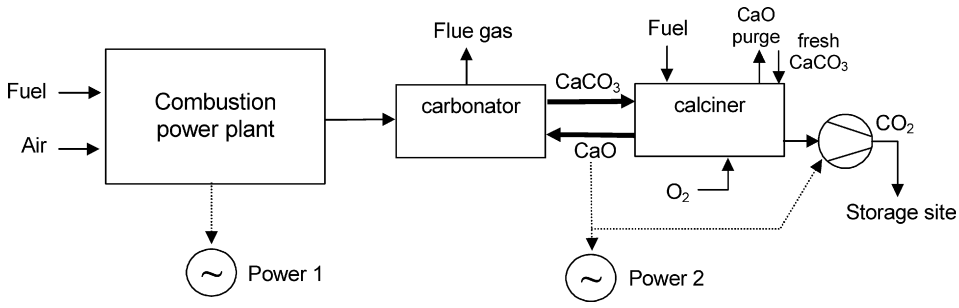

Fig. 1. Scheme of a carbonation/calcination loop (see Ref. [2] or case A in Ref. [3] for more details).

observed that the transition between the fast and slow regimes takes place quite suddenly at a given level of conversion and this level of conversion decreases when the number of carbonation/calcination cycles is increased. The evolution of the capture capacity of natural sorbents, over a number of cycles, has been studied in previous works [9,10] varying the process variables. It was found that capture capacity decreases dramatically during the first 20 cycles and then tends to stabilize to a residual conversion of around (7.5–8%), which remains constant up to at least 500 cycles [10]. Calcination temperatures over 950 °C, and/or extended calcination times accelerate sorbent degradation, and a residual capture capacity with a lower number of cycles is reached. Detailed observation by mercury porosimetry and SEM of the textural changes of the limestone throughout the cycling [9,11,12] concluded that the main mechanism of sorbent deactivation is the progressive sintering or grain growth of the originally rich texture of the material resulting from the first calcination. According to this mechanism, the $CaCO_3$ formed during carbonation will fill up all the available porosity made up of small pores plus a small fraction of the large voids, where the product layer grows until a critical thickness is reached marking the onset of the slow carbonation period. Second-order effects (pore mouth blockage, isolated voids in the calcined material, particle shrinkage) can also be detected in some special sorbents and conditions [12]. However, what marks the reduction in capture capacity is the grain sintering mechanism as the number of cycles increases combined with the modest product layer thickness allowed on the surface surrounding the large voids.

In all previous studies of capture capacity, the quantification of the carbonation rate during the initial fast reaction period under typical CO_2 absorber conditions (combustion flue gases at atmospheric pressure) has not been studied in detail. Kinetic data for the carbonation reaction have usually been adopted [2,3] from studies conducted with CaO particles that have undergone only one calcination cycle. However, it is reasonable to expect that the drastic textural changes behind the decay in sorbent capture capacity at the end of the fast carbonation period will also produce drastic changes in the carbonation rates. These rates are a critical parameter for the design and performance of the carbonation reactor. Therefore, an experimental study has been carried out to obtain information on reactivity for highly cycled lime particles that would represent the average sorbent particle in the proposed capture system. A basic reaction model was presented to interpret the reactivity data and chemical reaction constants that seem to be valid for a wide range of operating conditions and sorbent types were obtained.

2. Experimental

The cyclic carbonation and calcination reactions were experimentally studied in a thermo-gravimetric analyser (TGA) specially designed for long multicycle carbonation/calcination tests and to derive reactivity data during carbonation. Different variables affecting the carbonation process were studied in this work (particle diameter, limestone type, partial pressure of CO_2, carbonation temperature) in a series of calcinations/carbonation tests ranging from 10 to 100 s of cycles. The TGA consisted of a quartz tube placed inside a two-zone furnace capable of working at temperatures of up to 1000 °C. The temperature and sample weight were continuously recorded on computer. The reacting gas mixture (CO_2, O_2/air) was set by mass flow controllers and fed to the bottom of the quartz tube. A special characteristic in the design of this TGA was that the furnace had two zones capable of working at different temperatures. This furnace can be moved (by means of a pneumatic piston) up or down. The position with respect to the platinum basket alternates between calcination conditions (>850 °C) or carbonation conditions (around 650 °C). For each run in the TGA, around 15 mg of sorbent was introduced into the sample holder. Initial experiments were carried out to determine the total gas flow needed to eliminate external diffusion effects around the sample basket (this was finally set to 4×10^{-6} m^3/s which is about 0.06 m/s surface gas velocity around the sample basket at 650 °C, and 0.08 m/s surface gas velocity at 950 °C). Experiments were performed with an empty sample holder and an inert material in order to determine the disturbances in the weight readings when moving the furnace from the calcination to the carbonation position (a rapid change in temperature modifies the gas velocity around the sample basket). After correcting the data obtained from the previous blank tests, plots of conversion versus time for each cycle were made from the measured weight losses assuming that the CaO was converted to $CaCO_3$ during carbonation. At the end of each run, the samples were weighted in a different balance to check the accuracy of the TGA experiment. Good agreement was found in all the cases between the overall conversion calculated from the final weight difference and the conversion from the TGA. Although the TGA was designed to allow for rapid changes in temperature around the sample holder, there is still a delay in

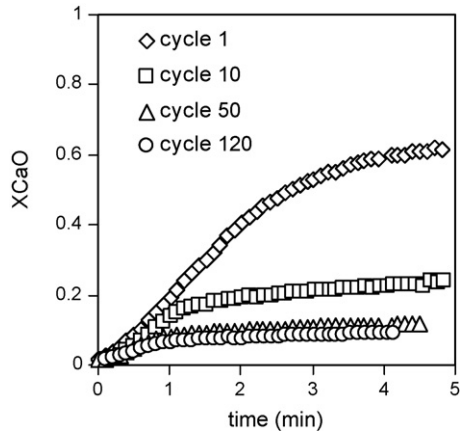

Fig. 2. Conversion curves vs. time for different cycle numbers. Limestone Piaseck; dp 0.4–0.6 mm; pCO_2 0.01 MPa; $T_{carbonation}$ 650 °C, for 5 min; $T_{calcination}$ 900 °C, for 5 min.

the order of 30–60 s before the desired carbonation temperature after each calcination step is reached. To stop the carbonation reaction during this temperature stabilization period, the flow of CO_2 was switched off until the carbonation temperature was stable to within a ±10 K difference with respect to the preset temperature.

3. Results and discussion

Fig. 2 shows the typical conversion curves versus time obtained during the experiments. The figure contains the curves corresponding to different cycles and, as can be seen, the main features characteristic of the carbonation reaction are present in all the cycles (initial fast reaction period followed by an abrupt change to a slower reaction stage). It is clear too, that although the maximum capture capacity decreases with the number of cycles, the path followed to reach the maximum conversion in each cycle is very similar. In these conditions, reaction times in the order of a couple of minutes are sufficient to reach the end of the fast reaction period but clear differences in the slope of these curves are also evident.

This work will be focus on particles that underwent a high number of cycles as these are representative of the average particle lifetime in the system of Fig. 1. Observation of these types of particles by mercury porosimetry and scanning electron microscopy, reported in previous works [9,11,12], indicate a change in pore structure from a complex network of pores of around 85–100 nm in diameter after the first calcination, to a much more open pore structure with pores of up to 1 μm in diameter after 100 s of cycles. Fig. 3(right) shows a characteristic sorbent pore structure after 30 cycles.

3.1. Effect of particle size

To investigate the possible effect of particle size on the carbonation reaction rate, four narrow particle size fractions (0.25–0.4, 0.4–0.6, 0.6–0.8 and 0.8–1 mm) of a limestone named "La Blanca" were tested in the TGA apparatus. Experimental results are plotted in Fig. 4. From previous studies on the carbonation reaction of CaO [6,8,13] it was expected that the particle size would have a strong effect on the overall particle carbonation rates. Particles with a pore structure similar to Fig. 3(left) were expected to show increasing resistance to CO_2 diffusion towards the free CaO surfaces in the interior of the particle as the particle sizes increased. Fig. 4(left) confirms this tendency, as it shows an example of the results obtained under the typical reaction conditions expected in the CO_2 absorber (650 °C and CO_2 volume fractions below 15%) and typical particle size ranges for fluidized bed systems. For the first calcination cycle, it can be concluded that diffusion effects inside the particle must be responsible for the slower carbonation rates of the larger particles. However, the quantitative differences in the slopes of the curves are modest, and only small differences in time were needed to achieve 50% conversion of particles (especially for the 0.25–0.4, 0.4–0.6 and 0.6–0.8 mm intervals). Furthermore, the maximum conversion attained was very similar for the particle range studied. This indicates that, the main rate resistance to CO_2 reacting with CaO was of a chemical nature.

Fig. 4(right) shows the conversion curve for cycle number 20. At this stage, sorbent capture capacity (conversion at the end of the fast reaction period) is lower, as expected, and the differences in slope for the fast reaction period between the different particle sizes have disappeared. This means that there are no diffusion effects in the interior of the particles and the reaction rate must be controlled by the reaction mechanism

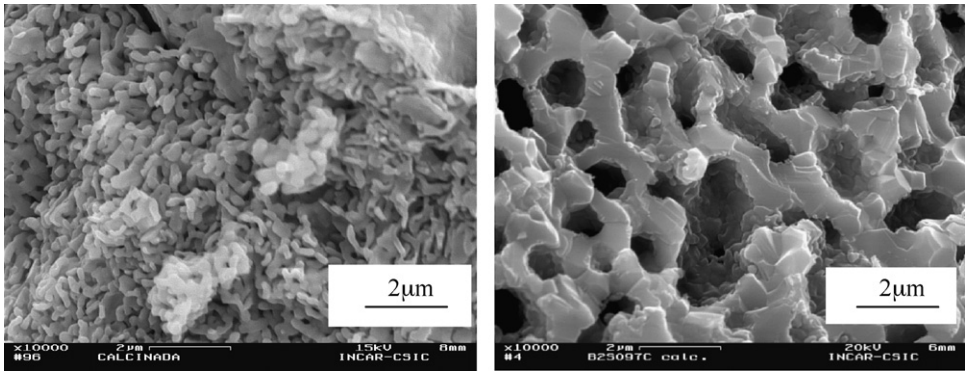

Fig. 3. View of the interior of a particle of CaO after one calcination (left) and after 30 carbonation/calcination cycles (right).

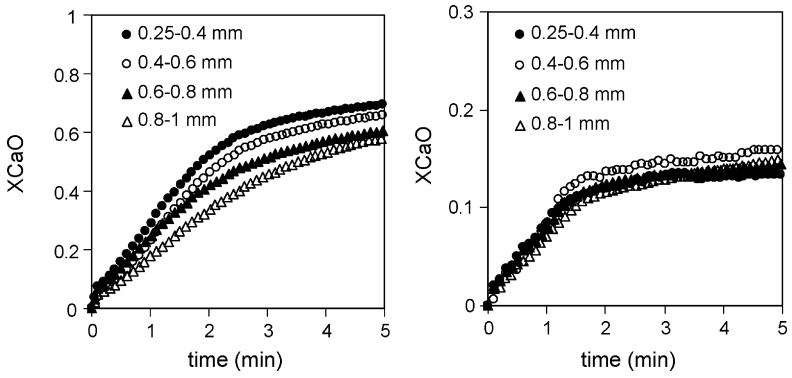

Fig. 4. Conversion curves vs. time for different particle size. Limestone: La Blanca, pCO_2 0.01 MPa, $T_{carbonation}$ 650 °C, for 20 min; $T_{calcination}$ 850 °C, for 15 min. (Left) cycle 1; (right) cycle 20. Note that the *Y*-axis scale is different for both figures.

taking place uniformly on a free surface of CaO. Therefore, a simple homogeneous carbonation model inside the particles can be expected to fit the reactivity data as discussed below.

3.2. Effect of limestone type

Different limestones generate very different textures on calcination and this can lead to different reaction patterns and maximum levels of conversion as is the case for the reaction of CaO with SO_2 [14]. However, the results reviewed in previous works [2,5–9,11,12] and applied to many cycles in a recent paper presented by this group [10], showed that there is a similarity in the decay trends of several limestones and that highly cycled samples present very similar pore structures. However, it is still necessary to elucidate the effect of limestone type on carbonation rates because other factors like the effect of impurities on the free surfaces of CaO could also yield different rate parameters. To study the effect of limestone type on the carbonation rates for an extended number of cycles, five different types of limestones were tested. As an example of the results obtained in the tests, the conversion curves for cycle number 40 are represented in Fig. 5.

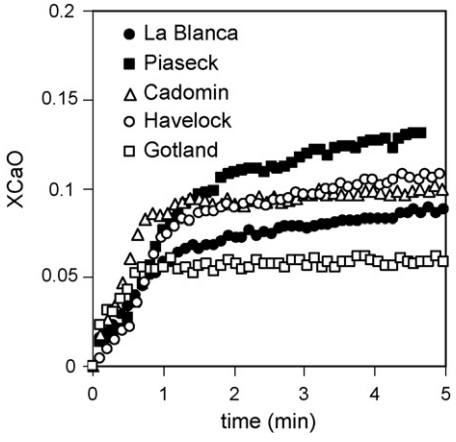

Fig. 5. Conversion curves vs. time for different limestone types. Particle size 0.4–0.6 mm, pCO_2 0.01 MPa, $T_{carbonation}$ 650 °C, for 20 min; $T_{calcination}$ 850 °C, for 15 min.

As can be seen in this figure, there are no appreciable differences in reactivity between the limestones tested. All the slopes during the fast carbonation period are similar. The small differences between limestones are more prominent during the slow carbonation stage, which is governed by the diffusion of the reactant through the product layer of $CaCO_3$ [8,15] which is not the subject of the present work. From a practical point of view, it is clear that, although differences in limestone performance do exist, they all behave in a similar way in terms of carbonation rate.

3.3. Effect of reaction atmosphere

The fast period in the carbonation reaction has been reported to correlate with reversible first-order kinetics [8] while the second slower carbonation stage has been reported to be independent of CO_2 partial pressures [8,15] except when close to equilibrium. Different carbonation/calcination tests were carried out by varying the CO_2 concentration in the reaction atmosphere, the pCO_2 ranging from 0.002 to 0.1 MPa. Fig. 6(left) shows the conversion curves obtained for the first cycle. It can be seen that the slopes of the fast carbonation reaction period are strongly affected by the concentration of the reactant. To prove the first-order of the reaction with respect to the CO_2, the relative carbonation rate ($\Delta X/\Delta t$ in min^{-1}) for the fast reaction period, was plotted against the CO_2 concentration in the reaction atmosphere. The linearity found in Fig. 6(right) is representative of an apparent first-order reaction with respect to the CO_2.

Fig. 7(left) and (right) represents the conversion curves for cycles 10 and 40, respectively. As can be seen, the trends observed are similar to the first cycle (Fig. 6(left)).

3.4. Effect of reaction temperature

The carbonation reaction was studied in a range of temperatures from 550 to 700 °C, close to the operation conditions in the proposed capture system. Fig. 8(left) and (right) shows the curves obtained for cycles 40 and 150, respectively. As can be seen, the slopes corresponding to the linear stage of the carbonation curve are very similar for the range of temperatures studied. This indicates the poor dependency of the kinetic parameter

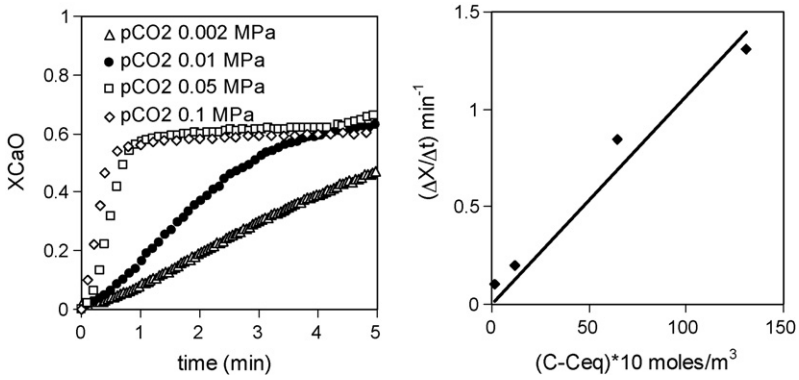

Fig. 6. (Left) Conversion curves vs. time for different pCO_2, cycle 1. Limestone: Piaseck, dp 0.4–0.6 mm, $T_{carbonation}$ 650 °C, 20 min; $T_{calcination}$ 900 °C, 15 min; (right) relative reaction rate vs. CO_2 concentration.

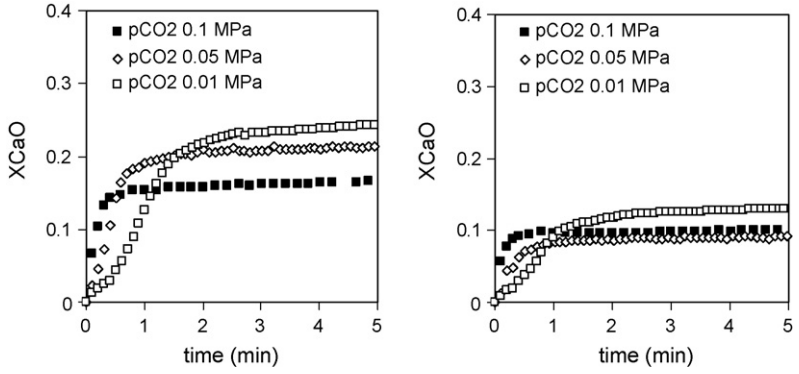

Fig. 7. Conversion curves vs. time for different pCO_2. Limestone: Piaseck, dp 0.4–0.6 mm, $T_{carbonation}$ 650 °C, 20 min; $T_{calcination}$ 900 °C, 15 min. (Left) cycle 10; (right) cycle 40.

on temperature in agreement with the results obtained in the literature [8,16,17].

3.4.1. Estimation of kinetic parameters

A fitting exercise was carried out to obtain kinetic constants for the carbonation reaction, using the entire experimental results with conditions ranging from $T_{carbonation}$ 550–700 °C; $T_{calcination}$ 850–950 °C; particle diameter 0.25–1 mm; pCO_2 0.01–0.1 MPa; sorbent type including five limestones and a dolomite and cycle numbers up to 500, of which Figs. 2–8 are only examples for specific conditions and a specific cycle number. The carbonation rate is described by the first-order Eq. (1), similar to the one used by earlier works referred to in Bhatia and Perlmuter [8] and consistent with a grain model for the carbonation reaction in the interior of the particle:

$$\frac{dX}{dt} = k_s S_N (1 - X)^{2/3} (C_{CO_2} - C_{eq}) \quad (1)$$

This form of rate expression was also used to model the behaviour of a fluidized CO_2 bed absorber [18]. In this equation, k_s represents the kinetic constant ($m^4/mol\,s$), X the CaO conversion, C_{CO_2} the CO_2 bulk concentration (mol/m^3) and C_{eq}

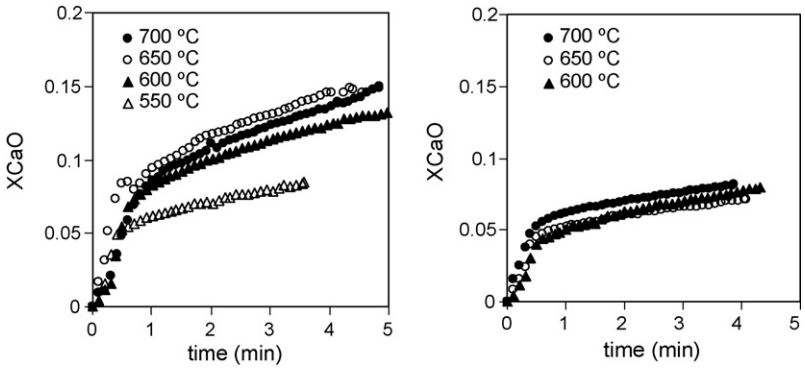

Fig. 8. Conversion curves vs. time for different $T_{carbonation}$. Limestone: Piaseck, dp 0.4–0.6 mm, pCO_2 0.01 MPa, $T_{calcination}$ 900 °C, 15 min. (Left) cycle 40; (right) cycle 150.

is the CO_2 concentration due to equilibrium (mol/m^3). S_N represents the surface area available for reaction in a particle cycled N times between calcination and carbonation conditions. This is simply proportional to the conversion of the particles at the end of the fast carbonation period, where an evenly distributed layer of $CaCO_3$ of 50 nm is assumed to have formed [11]. This layer thickness is much smaller than the pore diameter (which for highly cycled particles approaches 1 μm in diameter). Therefore, S_N has been estimated from the X_N (CaO conversion at the end of the fast reaction period of cycle N). It was assumed that the $CaCO_3$ product would form a 'flat' layer, h, of 50 nm thickness, on the reaction surface S_N (m^2/m^3 CaO), which was been estimated as follows:

$$S_N\left(\frac{m^2}{m^3}\right) = \frac{V_{M_{CaCO_3}} X_N}{M_{CaO} h}\rho_{CaO} \quad (2)$$

V_M being the molar volume of $CaCO_3$ (m^3/mol); X_N can be calculated trough Eq. (3), where X_r is equal to 0.075 and k equal to 0.52 for a wide range of sorbents and conditions [10], and N the number of carbonation/calcination cycles:

$$X_N = \frac{1}{1/(1-X_r)+kN} + X_r \quad (3)$$

M_{CaO} in Eq. (2) is the molecular weight of CaO, h the product layer thickness (m) and ρ_{CaO} is CaO density (m^3/kg CaO). Other pore geometries will require different equations to estimate S_N [11].

Eq. (2) yields surface areas of 1.0–2.0 10^6 m^2/m^3 for highly cycled samples. The values obtained for the rate constant, k_s in Eq. (1), varied between: 3.2 and 8.9×10^{-10} m^4/mol s. This must be an intrinsic kinetic parameter, since intraparticle and transport resistances were insignificant under the conditions studied. The central value of this interval (6.05×10^{-10}) is remarkably close to the value, $k_s = 5.95 \times 10^{-10}$ m^4/mol s obtained by Bhatia and Perlmuter for lime (one calcination only) using their pore model [8]. The pore model yielded similar values of k_s ($3.1–8.7 \times 10^{-10}$ m^4/mol s) when assuming reasonable structural parameters for the pores (pore diameter, and total pore length, L) to calculate the parameter Ψ (being $\Psi = 4\pi L_N/{S_N}^2$, the subscript N means that the values refer to cycle N):

$$\frac{dX}{dt} = k_s S_N (C_{CO_2} - C_{eq})(1-X)\sqrt{1-\Psi \ln(1-X)} \quad (4)$$

In this equation, X, S_N, C_{CO_2} and C_{eq} represent the same parameters as in Eq. (1). To derive the kinetic parameters, only experimental data conversion clearly in the fast reaction stage (up to conversions 70–80% of X_N) were considered. The integrated forms of Eqs. (1) and (4) were used to find the k_s that yielded the least-square errors between experimental and calculated conversions. The carbonation rate parameters obtained in this work need to be put in the context of ongoing developments in order to design a full carbonation/calcination pilot system following the scheme in Fig. 1. The reaction rates measured for particles cycled a high number of times, the fact that they follow a homogenous reaction model during their carbonation, and the range of intrinsic reaction constants obtained suggest that fluidized bed systems can be effective absorbers for capturing the CO_2 present in the flue gases from power plants, even when the particles in the bed have experienced many carbonation calcination cycles. Fluidized bed reactors can accommodate solid residence times of several minutes, axial hold ups of several hundreds of kg/m^2 and solid circulation rates in the order of 10 kg/m^2 s of CaO (equivalent molar flow of approximately 180 mol CaO/m^2 s). This large flow of CaO should be able to match the poor conversion of CaO to $CaCO_3$ and still capture a relevant fraction of the CO_2 in the flue gas flowing through a CFB CO_2 absorber (as an example, with spatial velocities of 6 m/s at 650 °C and 15 vol.% CO_2 there are 13 mol CO_2/m^2 s). Therefore, a range of reasonable operating conditions for the absorber, not far from the standard in existing large scale circulating fluidized bed systems, should allow an effective CO_2 capture from the flue gas from a power plant in a system similar to the one depicted in Fig. 1. Experimental work in Europe and in Canada is being carried out to demonstrate on a continuous laboratory scale, this CO_2 capture concept of a fully interconnected fluidized bed carbonator–calciner system.

4. Conclusions

Multicycle carbonation/calcination experiments were carried out to determine kinetic constants for the carbonation reactions in the fast carbonation periods that occur in every cycle. This work has focused on particles being cycled a high number of times in the system, kinetic constants were estimated by means of a simple equation and the values obtained were found to be in close agreement with the values in the 1983 paper by Bathia and Perlmutter. The carbonation reaction rates seem to be suited to the range of residence times typical of circulating fluidized beds.

Acknowledgements

This work is partially funded by the European Commission (C3-Capture), the Spanish Ministry of Education ("Juan de la Cierva" program) and Industry, with the CENIT-CO2 project partially funded by Unión Fenosa S.A. The help from D. Alvarez in obtaining the SEM photographs is also acknowledged.

References

[1] B. Metz, O. Davidson, H. de Coninck, M. Loos, L. Meyer (Eds.). Special Report on Carbon Dioxide Capture and Storage, Intergovernmental Panel on Climate Change, Cambridge University Press, 2005.
[2] T. Shimizu, T. Hirama, H. Hosoda, K. Kitano, M. Inagaki, K. Tejima, A twin fluid-bed reactor for removal of CO_2 from combustion processes, Trans. IChemE 77A (1999) 62–68.
[3] J. Wang, E.J. Anthony, J.C. Abanades, Clean and efficient use of petroleum coke for combustion and power generation, Fuel 83 (2004) 1341–1348.
[4] J.C. Abanades, E.J. Anthony, J. Wang, J.E. Oakey, Fluidized bed combustion systems integrating CO_2 capture with CaO, Environ. Sci. Technol. 39 (2005) 2861–2866.
[5] G.P. Curran, C.E. Fink, E. Gorin, Carbon dioxide-acceptor gasification process: studies of acceptor properties, Adv. Chem. Serv. 69 (1967) 141–165.

[6] A. Silaban, D.P. Harrison, High-temperature capture of carbon dioxide: characteristics of the reversible reaction between CaO(s) and CO_2(g), Chem. Eng. Commun. 137 (1995) 177–190.
[7] R. Barker, The reversibility of the reaction $CaCO_3 = CaO + CO_2$, J. Appl. Chem. Biol. 23 (1973) 733–742.
[8] S.K. Bathia, D.D. Perlmutter, Effect of the product layer on the kinetics of the CO_2-lime reaction, AIChE J. 39 (1983) 79–86.
[9] J.C. Abanades, D. Alvarez, Conversion limits in the reaction of CO_2 with lime, Energy Fuels 17 (2003) 308–315.
[10] G.S. Grasa, J.C. Abanades, CO_2 capture capacity of CaO in long series of carbonation/calcination cycles, Ind. Eng. Chem. Res. 45 (2006) 8846–8851.
[11] D. Alvarez, J.C. Abanades, Determination of the critical product layer thickness in the reaction of CaO with CO_2, Ind. Eng. Chem. Res. 44 (2005) 5608–5615.
[12] D. Alvarez, J.C. Abanades, Pore-size and shape effects on the recarbonation performance of calcium oxide submitted to repeated calcination/recarbonation cycles, Energy Fuels 19 (2005) 270–278.
[13] J.S. Dennis, A.N. Hayhurst, The effect of CO_2 on the kinetics and extent of calcination of limestone and dolomite particles in fluidised beds, Chem. Eng. Sci. 42 (1987) 2361–2372.
[14] E.J. Anthony, D.L. Granatstein, Sulfation phenomena in fluidised bed combustion systems, Prog. Energy Combust. Sci. 27 (2001) 215–236.
[15] D. Mess, A.F. Sarofim, J.P. Longwell, Product layer diffusion during the reaction of calcium oxide with carbon dioxide, Energy Fuels 13 (1999) 999–1005.
[16] M. Ahiara, T. Nagai, J. Matsushita, Y. Negishi, H. Ohya, Development of porous solid reactant for thermal-energy storage and temperature upgrade using carbonation/decarbonation reaction, Appl. Energy 69 (2001) 225–238.
[17] A.J. Dedman, A.J. Owens, Calcium cyanamide synthesis. Part 4. The reaction $CaO + CO_2 = CaCO_3$, Trans. Faraday Soc. 58 (1962) 2027–2035.
[18] J.C. Abanades, E.J. Anthony, D.Y. Lu, C. Salvador, D. Alvarez, Capture of CO_2 from combustion gases in a fluidized bed of CaO, AIChE J. 50 (2004) 1614–1622.